

Supplementary Information

Interfacial Polymerization of MOF “Monomer” to Fabricate Flexible and Thin

Membrane for Molecular Separation with Ultrafast Water Transport

Xiaolei Cui¹, Guodong Kong¹, Yang Feng¹, Longting Li³, Weidong Fan¹, Jia Pang¹, Lili Fan¹, Rongming Wang¹, Hailing Guo³, Zixi Kang^{1,2,*} and Daofeng Sun^{1,*}

¹ College of Science, School of Materials Science and Engineering, China University of Petroleum (East China), Qingdao, Shandong, 266580, PR China

² State Key Laboratory of Structural Chemistry, Fujian Institute of Research on the Structure of Matter, Chinese Academy of Sciences, Fuzhou, Fujian, 350002, PR China.

³ College of Chemical Engineering, China University of Petroleum (East China), Qingdao, Shandong, 266580, PR China

*Corresponding authors. Email: kzx@upc.edu.cn; dfsun@upc.edu.cn

Supporting Figures and Tables

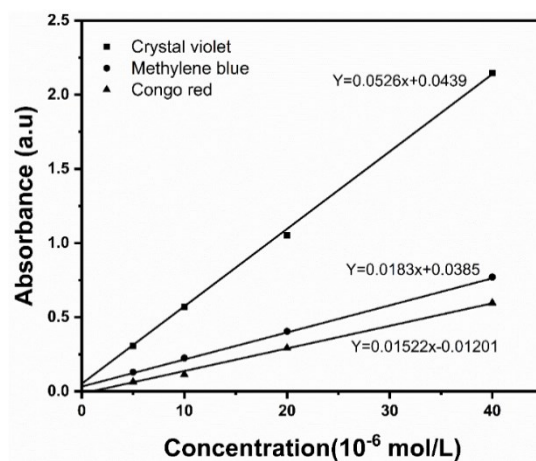


Figure S1. The standard curves of crystal violet, methylene blue and Congo red.

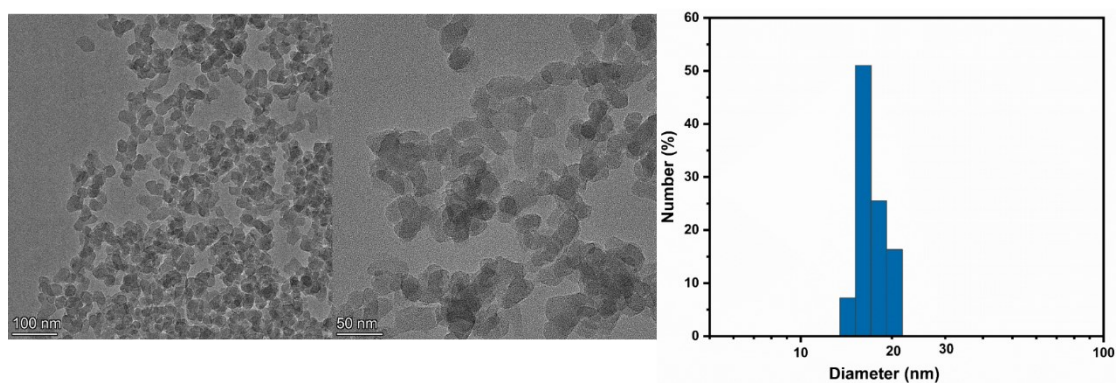


Figure S2. TEM and size statistics of S-UiO-66-NH₂.

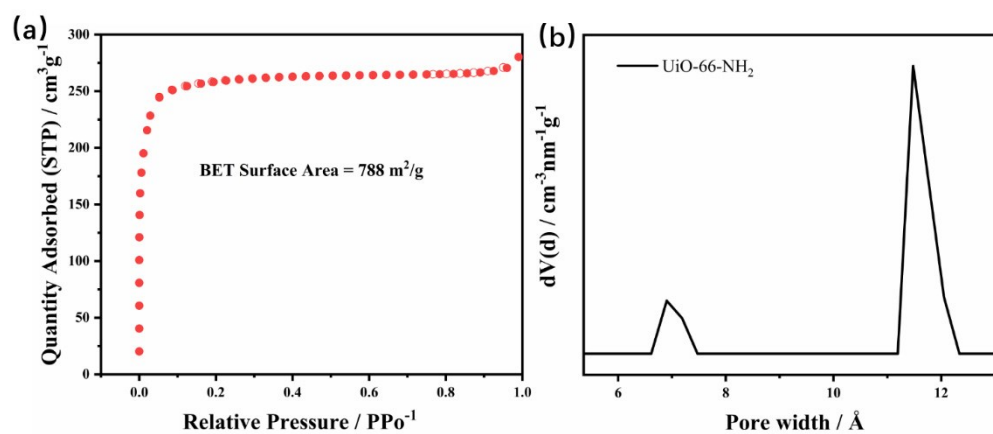


Figure S3. The N₂ adsorption results: (a) the N₂ adsorption-desorption isotherms and BET surface area at 77 K for UiO-66-NH₂ “monomer”, (b) the pore size distribution of UiO-66-NH₂ “monomer”.

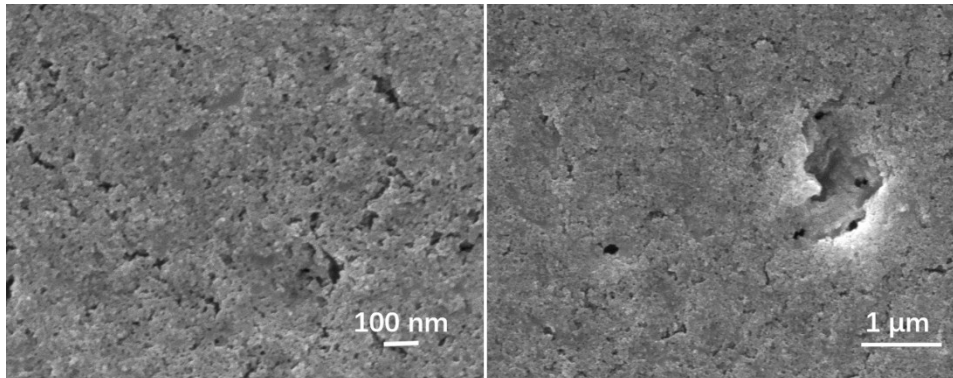


Figure S4. SEM images of the UiO-66-NH₂-TMC membrane fabricated by conventional liquid-liquid interface polymerization method in the preliminary experiment.

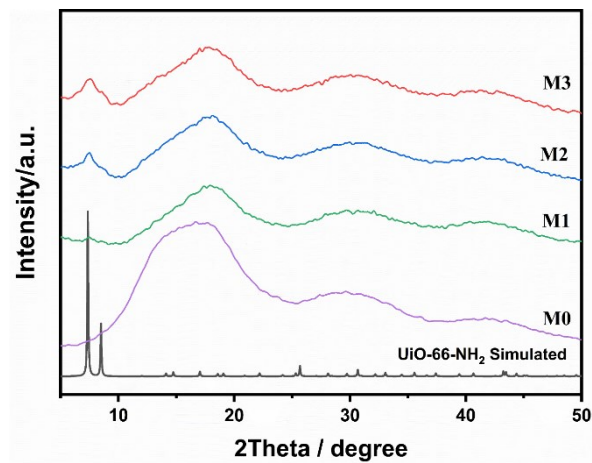


Figure S5. XRD of UiO-66-NH₂-TMC membranes. M0: PES substrate; M1, M2, M3: membranes prepared with UiO-66-NH₂ “monomer” concentrations of 0.03 wt%, 0.05 wt% and 0.1 wt% respectively.

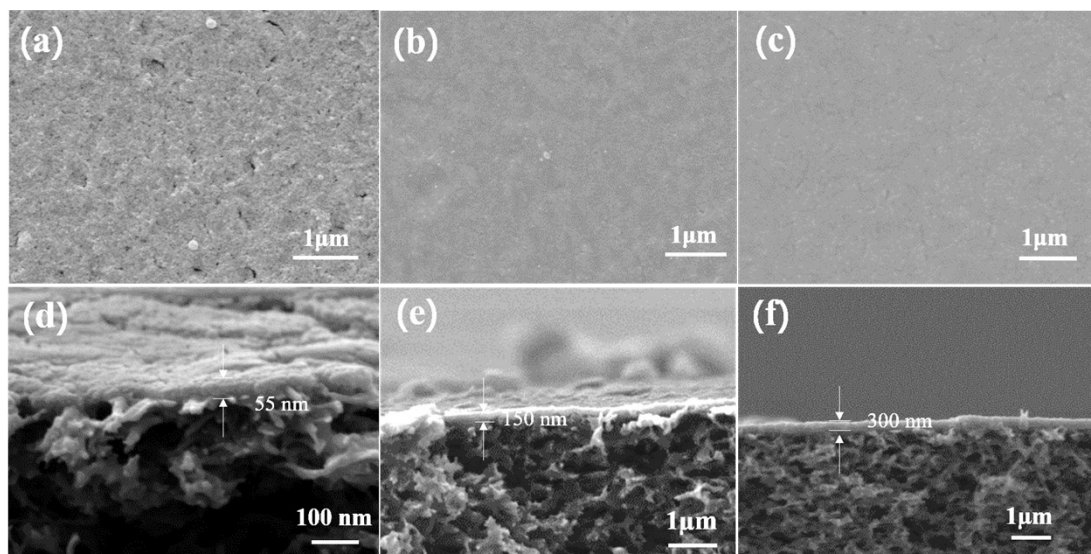


Figure S6. The top-view and cross-section SEM images of (a, d) M1, (b, e) M2 and (c, f) M3.

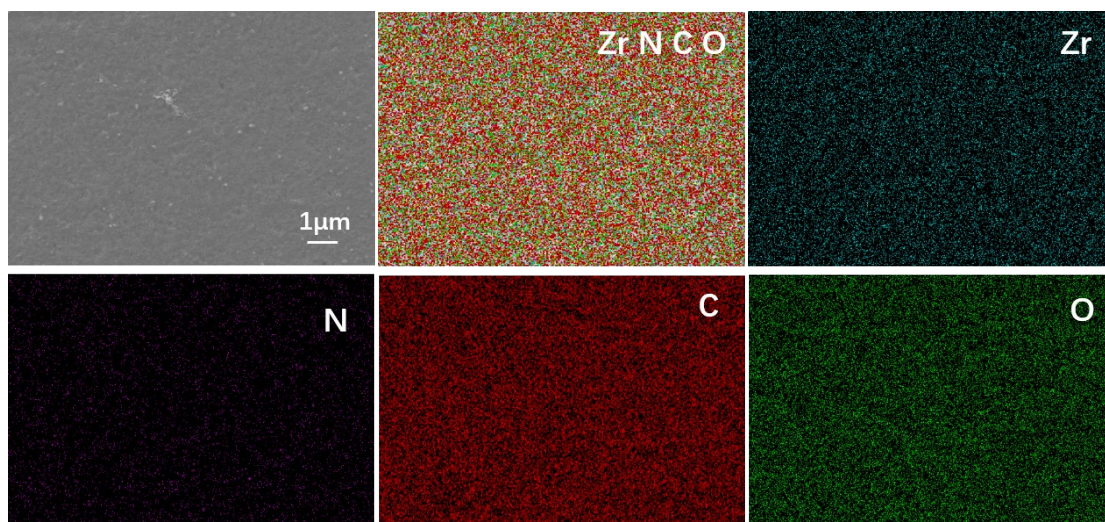


Figure S7. EDS mapping images of UiO-66-NH₂-TMC membrane.

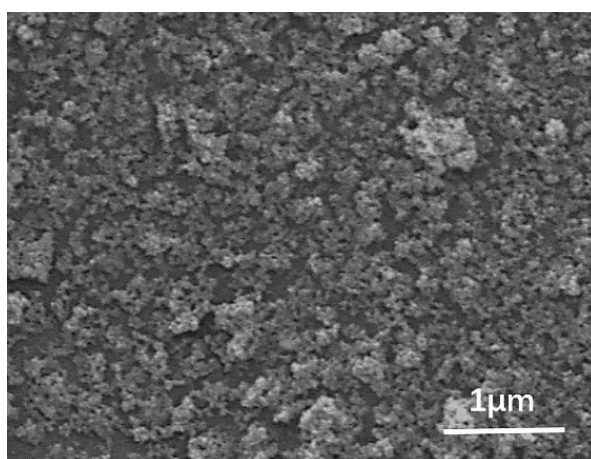


Figure S8. The top-view SEM image of UiO-66-TMC membrane.

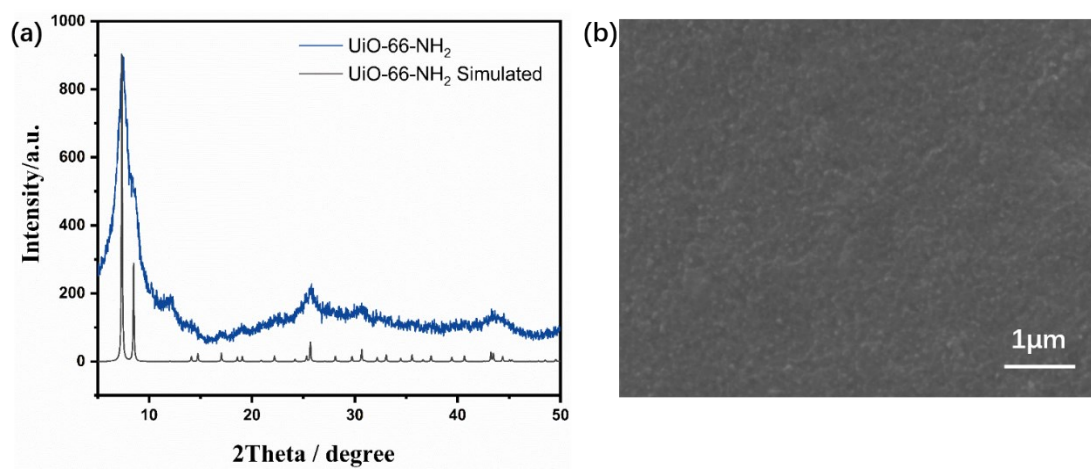


Figure S9. (a) The PXR D pattern of UiO-66-NH₂ after soaked in water for 30 days; (b) SEM image of the membrane prepared with the UiO-66-NH₂ after soaked in water for 30 days.

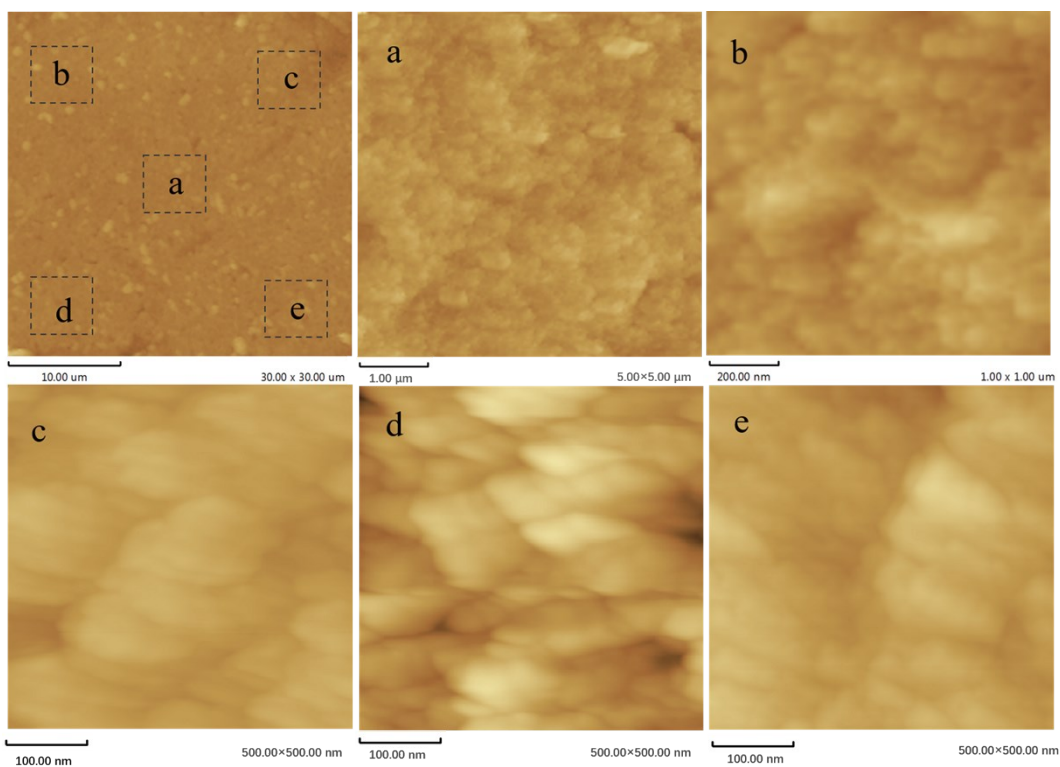


Figure S10. The AFM images of M2 and magnified of region a-e in M2.

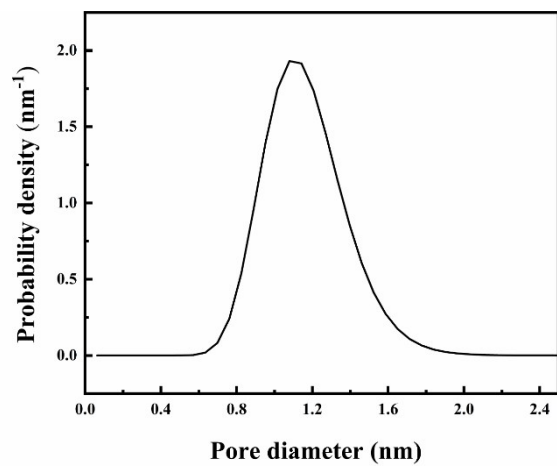


Figure S11. The pore size distribution of UiO-66-NH₂-TMC membrane.

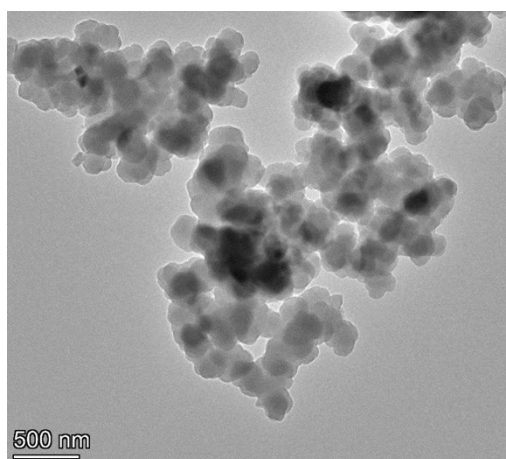


Figure S12. TEM of the L-UiO-66-NH₂.

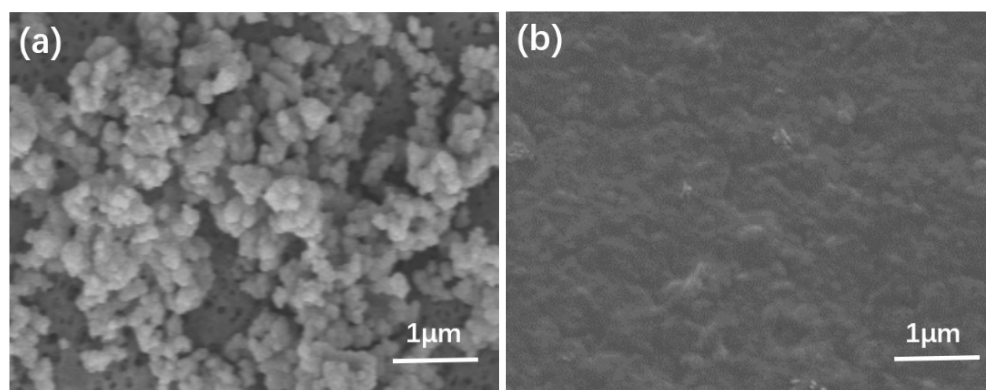


Figure S13. The top-view SEM images of (a) L-UiO-66-NH₂-TMC membrane and (b) M2 membrane.

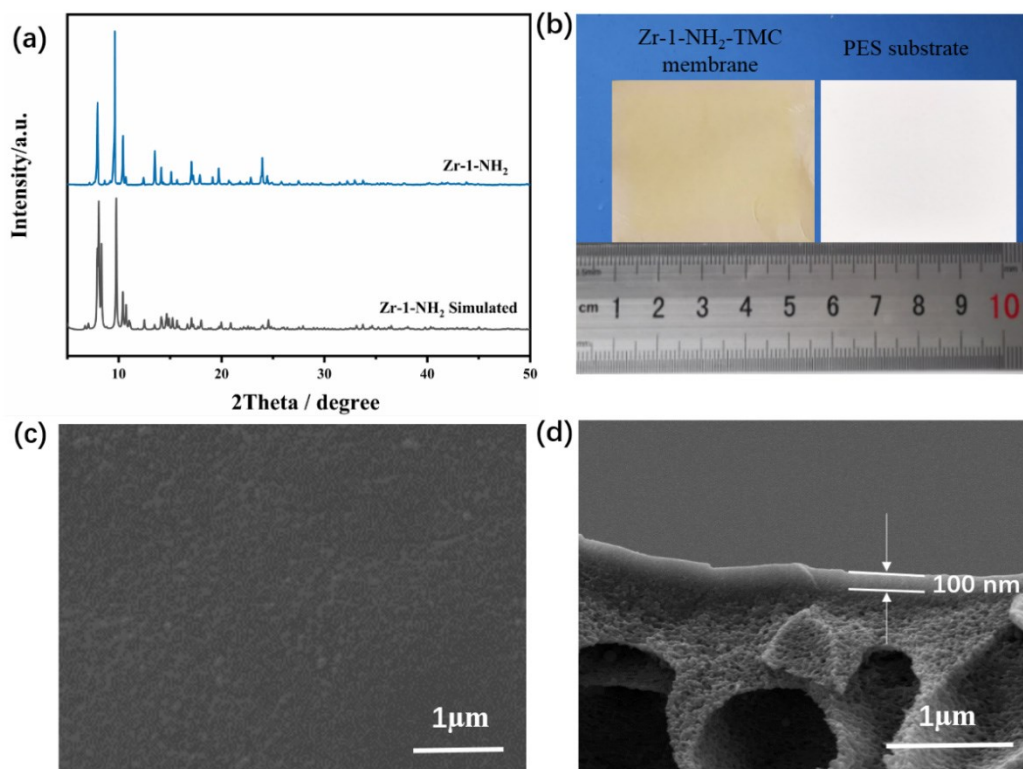


Figure S14. (a) PXRD of Zr-1-NH₂ “monomer”, (b) photograph of Zr-1-NH₂-TMC membrane and PES substrate, (c) the top-view SEM image of Zr-1-NH₂-TMC membrane, (d) the cross-section SEM image of the Zr-1-NH₂-TMC membrane.

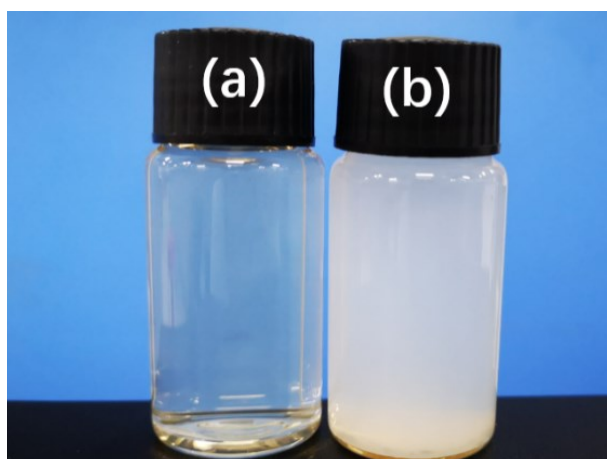


Figure S15. (a) UiO-66-NH₂ “monomer” diluted directly in deionized water after synthesis, (b) UiO-66-NH₂ “monomer” was dried and then diluted in deionized water after synthesis.

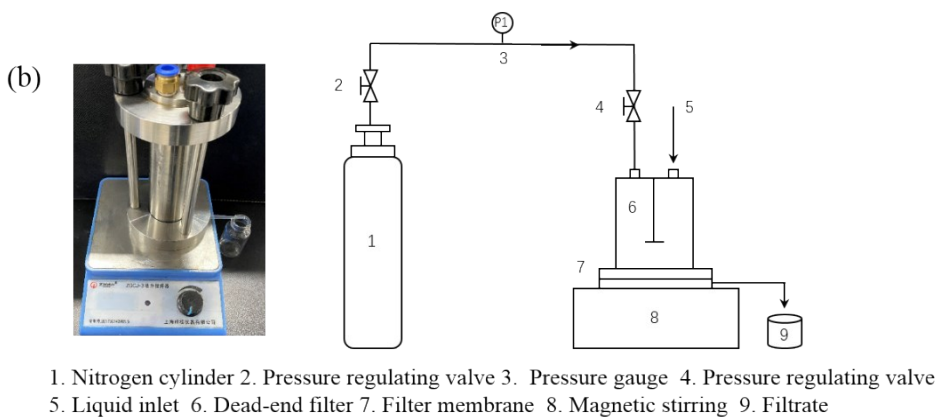
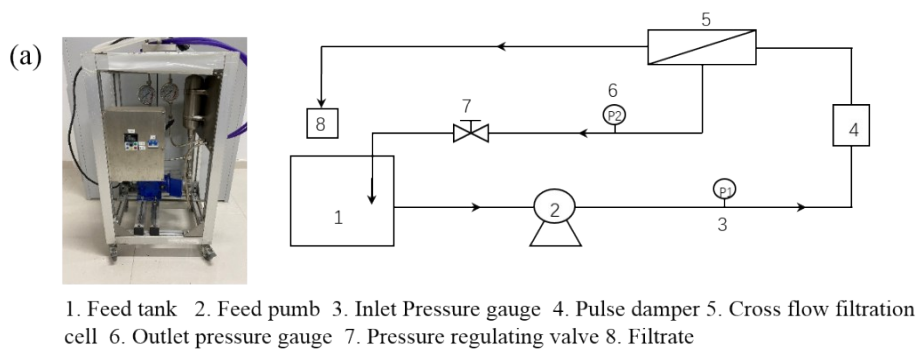


Figure S16. Photograph and schematic illustration of nanofiltration devices for (a) cross-flow mode and (b) dead-end mode.

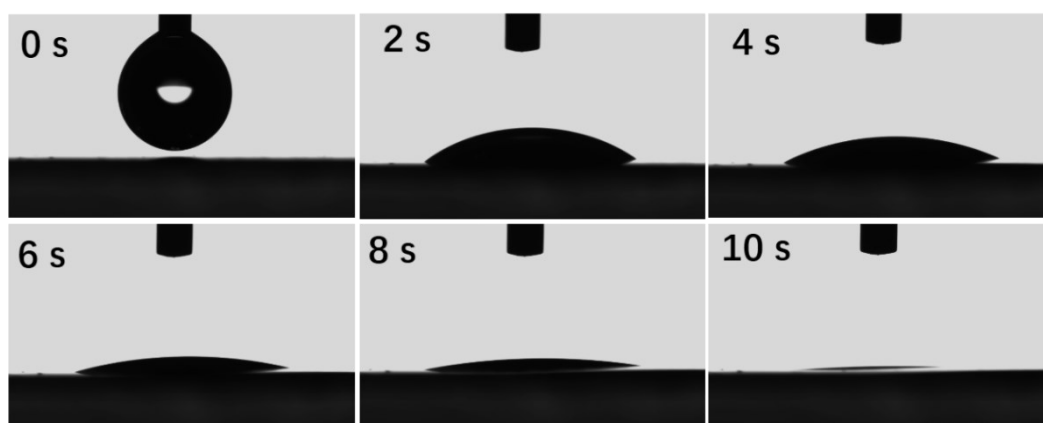


Figure S17. The water contact angle of M2 changes with time.

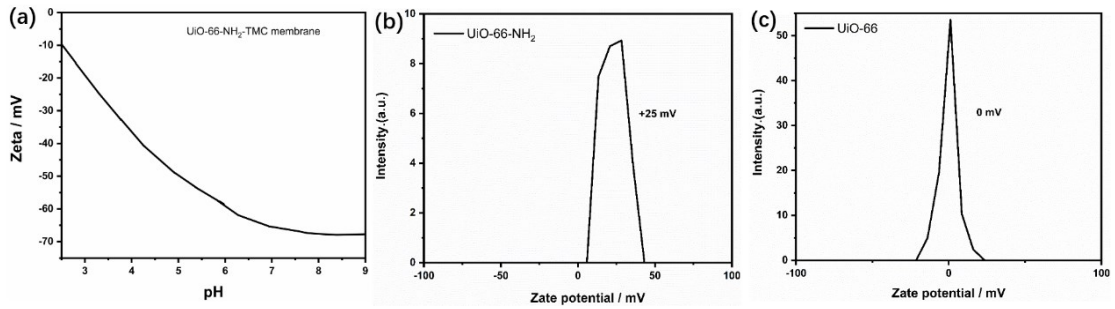


Figure S18. Zeta potential of (a) UiO-66-NH₂-TMC membrane as a function of solution pH, (b) UiO-66-NH₂ "monomer" aqueous solution and (c) UiO-66 aqueous solution.

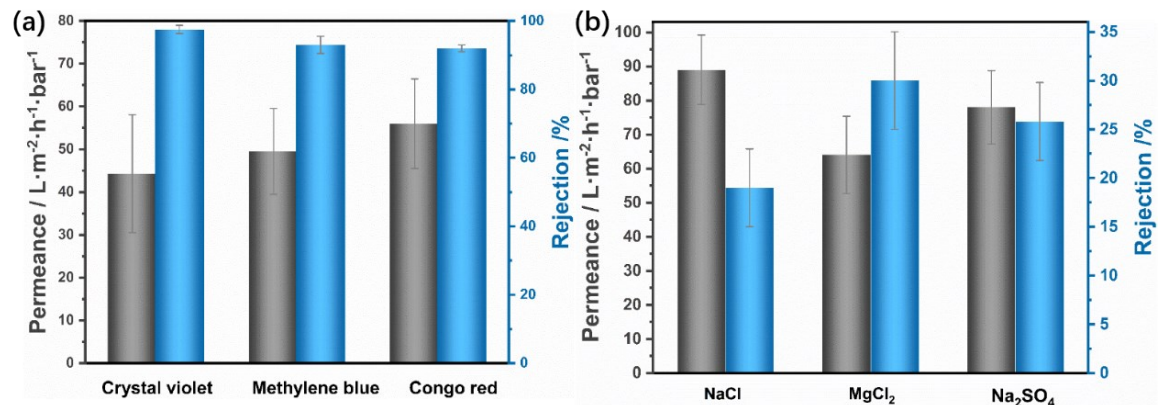


Figure S19. The nanofiltration performance of (a) three dyes (50 ppm) and (b) three salt solutions (1000 ppm) on M2.

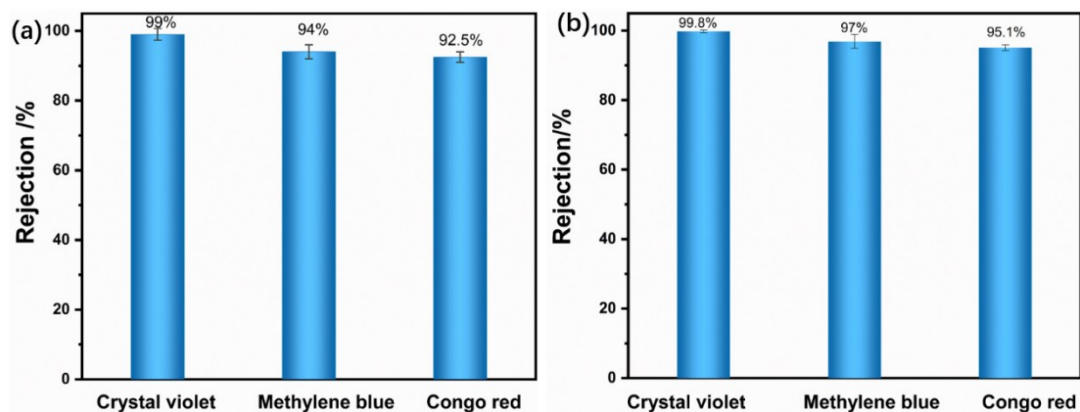


Figure S20. The nanofiltration performance of M2 under the (a) dye interference (mixture of 10 ppm crystal violet, methylene blue and Congo red) and (b) organic matter interference (10 ppm crystal violet, methylene blue, Congo red and 0.1g L⁻¹ BSA).

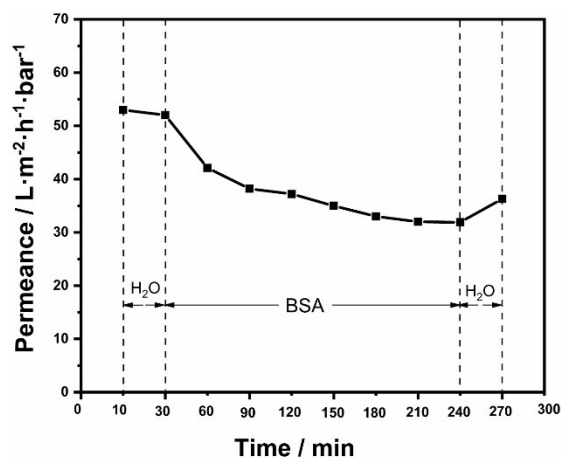


Figure S21. Time-dependent permeance for M2 membrane during filtration of BSA.

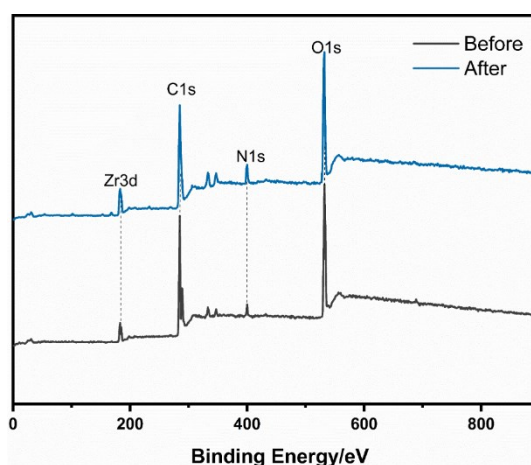


Figure S22. The XPS results for the M2 before and after nanofiltration test.

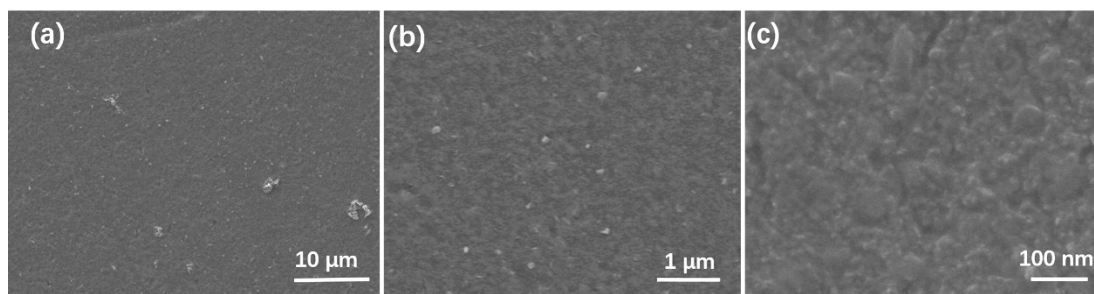


Figure S23. SEM images with different magnification for the UiO-66-NH₂-TMC membrane after bending test.

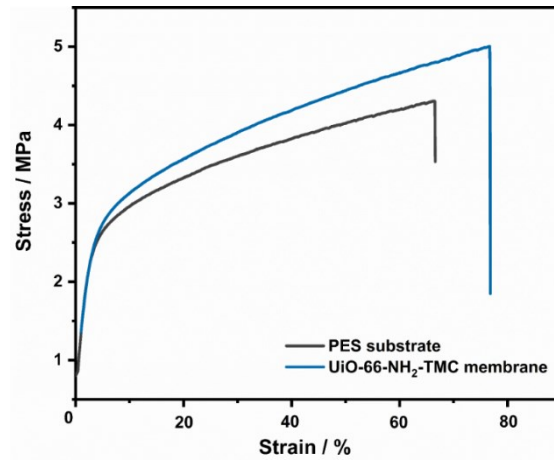


Figure S24. The tensile tests of UiO-66-NH₂-TMC and PES membrane.

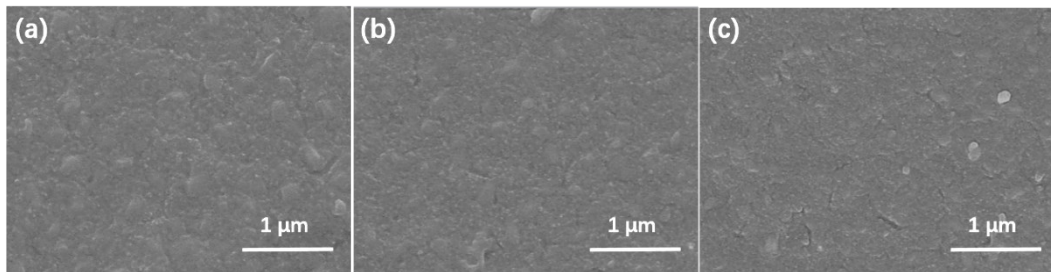


Figure S25. The top-view SEM images of region a-c in the large-area membrane.

Table S1. MOF ratio in the composite membrane

Membrane	MOF mass (g)	TMC mass(g)	MOF ratio (%)
M1	0.00086	0.00222	27.9
M2	0.00295	0.00234	55.8
M3	0.00760	0.00290	72.4

Table S2. Cost estimate of UiO-66-NH₂-TMC selective layer.

	UiO-66-NH ₂		TMC	cyclohexane
	2-aminoterephthalic acid	ZrCl ₄		
Price (USD g ⁻¹)	1.7	2.2	4.3	2
Dosage (g m ⁻²)	0.7	1	5.7	1100
Cost (USD m ⁻²)	1	2	25	2
Total (USD m ⁻²)		30		

Table S3. The structural properties of dye molecules in this study.

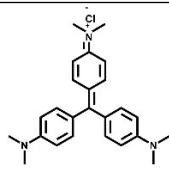
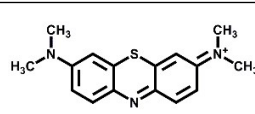
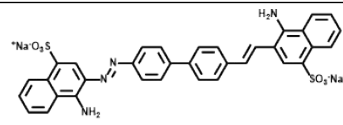
	Crystal violet	Methylene blue	Congo Red
Chemical structure			
Size (Å)	13.05×13.05	13.17×5.27	25.60×7.30
Mol. wt. (g mol ⁻¹)	373.53	319.85	696.68
Charge	Positive	Positive	Negative

Table S4. The content of Zr in feed and permeate solution.

Solution	Measured element	Contents (mg/L)	Dissolved MOF (mg)
Feed	Zr	0.0045±0.0015	0.00042±0.00014
Permeate	Zr	0.0057±0.0009	0.00053±0.00008

Table S5. The water permeance and dye rejection rate of reported membranes.

Membrane	Dye	Water permeance (L m ⁻² h ⁻¹ bar ⁻¹)	Rejection rate (%)	Reference
PA/UiO-66	Rose Bengal	15.4	100	1
PA/UiO-66	Azithromycin	15.4	97.6	1
PM TFN membrane	Methyl blue	13.09	99.9	2
PA/ZIF-8	Congo red	2.71	99.8	3
UiO-66/PGP	Methyl orange	31.33	94.84	4
Zif-8/PSS	Methyl blue	26.5	98.6	5
UiO-66	Methyl blue	0.77	99.8	6
ZIF-8	Rose Bengal	37.5	98	7
UiO-66-NH ₂ -based MMMs	Rhodamine B	34	92	8
ZIF-8/PEI hybrid membrane	Methyl blue	33	99.6	9
ZIF-8/PES	Rose bengal	1.3	99	10
UiO-66@GO/PES	Methyl orange	15.7	88.6	11
UiO-66-(COOH)/prGO	Methylene blue	20	92.55	12
Sm-MOF/GO	Rrhodamine B and Methylene blue	26	>91%	13
PA-ZIF-93	Acridine orange	0.24	98	14
BUT-8/PEI-HPAN-50	Methylene blue	51	98.3	15
UiO-66-NH ₂ -TMC	Crystal violet	55.9	99.8	This work

Supporting references

- 1 X. Cheng, X. Jiang, Y. Zhang, C. H. Lau, Z. Xie, D. Ng, S. J. D. Smith, M. R. Hill and L. Shao, *ACS Appl. Mater. Interfaces* 2017, **9**, 38877-38886.
- 2 P. Zhao, R. Li, W. Wu, J. Wang, J. Liu and Y. Zhang, *Compos. B. Eng.* 2019, **176**, 107208.
- 3 L. Wang, M. Fang, J. Liu, J. He, J. Li and J. Lei, *ACS Appl. Mater. Interfaces* 2015, **7**, 24082-24093.
- 4 S. Y. Fang, P. Zhang, J. L. Gong, L. Tang, G. M. Zeng, B. Song, W. C. Cao, J. Li and J. Ye, *Chem. Eng.J.* 2020, **385**, 123400.
- 5 R. Zhang, S. Ji, N. Wang, L. Wang, G. Zhang and J.R. Li, *Angew. Chem. Int. Ed.* 2014, **53**, 9775-9779.
- 6 X. Wang, L. Zhai, Y. Wang, R. Li, X. Gu, Y. D. Yuan, Y. Qian, Z. Hu and D. Zhao, *ACS Appl. Mater. Interfaces* 2017, **9**, 37848-37855.
- 7 Y. Li, L. H. Wee, J. A. Martens and I. F. J. Vankelecom, *J. Membr. Sci.* 2017, **523**, 561-566.
- 8 F. Aghili, A. A. Ghoreyshi, A. Rahimpour and B. Van der Bruggen, *Ind. Eng. Chem. Res.* 2020, **59**, 7825-7838.
- 9 L. Yang, Z. Wang and J. Zhang, *J. Membr. Sci.* 2017, **532**, 76-86.
- 10 Y. Li, L. H. Wee, A. Volodin, J. A. Martens and I. F. J. Vankelecom, *ChemComm* 2015, **51**, 918.
- 11 J. Ma, X. Guo, Y. Ying, D. Liu and C. Zhong, *Chem. Eng.J.* 2017, **313**, 890-898.
- 12 P. Zhang, J. L. Gong, G. M. Zeng, B. Song, H. Y. Liu, S. Y. Huan and J. Li, *Chemosphere* 2018, **204**, 378-389.
- 13 G. Yang, D. Zhang, G. Zhu, T. Zhou, M. Song, L. Qu, K. Xiong and H. Li, *RSC Adv.* 2020, **10**, 8540-8547.
- 14 C. Echaide-Górriz, J. A. Zapata, M. Etxeberría-Benavides, C. Téllez and J. Coronas, *Sep. Purif. Technol.* 2020, **236**.
- 15 Y. Meng, L. Shu, L. Liu, Y. Wu, L. H. Xie, M. J. Zhao and J. R. Li, *J. Membr. Sci.* 2019, **591**, 117360.